

Infrared Action Spectroscopy of Nitrous Oxide on Cationic Gold and Cobalt Clusters

Supporting Information

Ethan M. Cunningham¹, Alice E. Green¹, Gabriele Meizyte¹, Alexander S. Gentleman¹, Peter W. Beardsmore¹, Sascha Schaller², Kai M. Pollow³, Karim Saroukh³, Marko Förstel³, Otto Dopfer^{3*}, Wieland Schöllkopf³, André Fielicke^{2,3*} & Stuart R. Mackenzie^{1*}

1. Department of Chemistry, University of Oxford, Physical and Theoretical Chemistry Laboratory, South Parks Road, Oxford OX1 3QZ, United Kingdom
2. Fritz-Haber-Institut der Max-Planck-Gesellschaft, Faradayweg 4–6, 14195 Berlin, Germany
3. Institut für Optik und Atomare Physik, TU Berlin, Hardenbergstr. 36, 10623 Berlin, Germany

Contents

Time-of-Flight Mass Spectra	2
Simulated Infrared Spectra	4
Au(N ₂ O) ⁺	4
Au ₂ (N ₂ O) ⁺	5
Au ₅ (N ₂ O) ⁺	6
Co ₄ (N ₂ O) ⁺	7
Co ₅ (N ₂ O) ⁺	9
Calculated Structures	10
Au _n (N ₂ O) ⁺	10
Au ₂ (N ₂ O) ⁺	10
Au ₃ (N ₂ O) ⁺	11
Au ₄ (N ₂ O) ⁺	12
Au ₅ (N ₂ O) ⁺	13
Co _n (N ₂ O) ⁺	14
Co ₂ ⁺ (N ₂ O) ⁺	14
Co ₃ (N ₂ O) ⁺	15
Co ₄ (N ₂ O) ⁺	16
Co ₅ (N ₂ O) ⁺	18
Bond Lengths	
(N ₂ O)	19
Au _n (N ₂ O) ⁺	19
Co _n (N ₂ O) ⁺	21
References	23

Time-of-Flight Mass Spectra

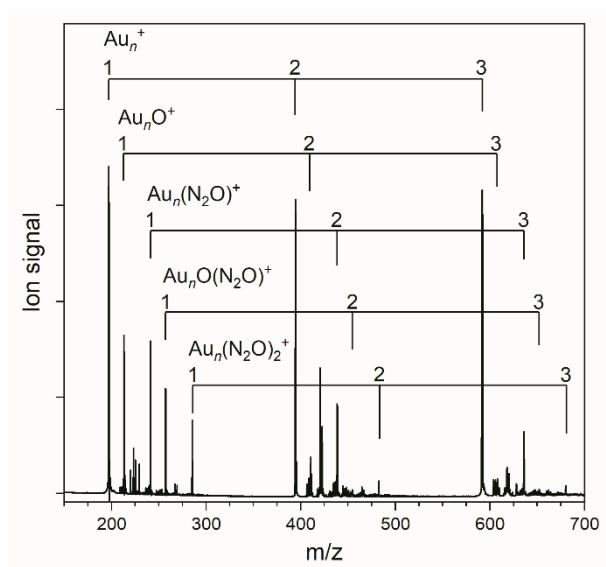


Figure S1. Time-of-flight mass spectrum illustrating the production of Au_n^+ and Au_nO^+ ($n = 1-3$) clusters with attached nitrous oxide obtained following laser ablation of a gold rod in the presence of a helium carrier gas (10 bar backing pressure) and reaction gas of N_2O delivered downstream *via* the reaction channel.

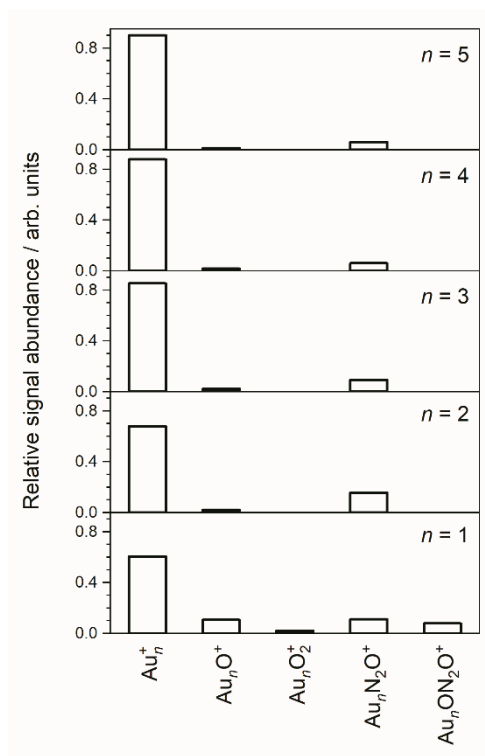


Figure S2. Bar graph illustrating the relative abundances of each of the ion signals (from the time-of-flight mass spectrum) Au_n^+ , Au_nO^+ , Au_nO_2^+ , $\text{Au}_n\text{N}_2\text{O}^+$, and $\text{Au}_n\text{ON}_2\text{O}^+$ ($n = 1-5$).

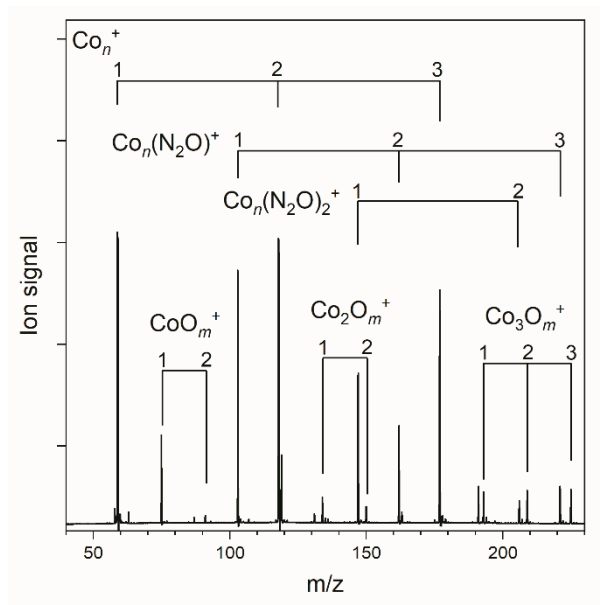


Figure S3. Time-of-flight mass spectrum illustrating the production of Co_n^+ ($n = 1-3$) with attached nitrous oxide and Co_nO_m^+ ($n = 1-3$; $m = 1-3$) obtained following laser ablation of a cobalt rod in the presence of a helium carrier gas (10 bar backing pressure) and reaction gas of N_2O delivered downstream *via* the reaction channel.

Simulated Infrared Spectra

Simulated spectra are illustrated together with the experimental IR-MPD spectra, and are scaled by a factor of 0.955, derived from the stretching frequencies of isolated nitrous oxide.¹

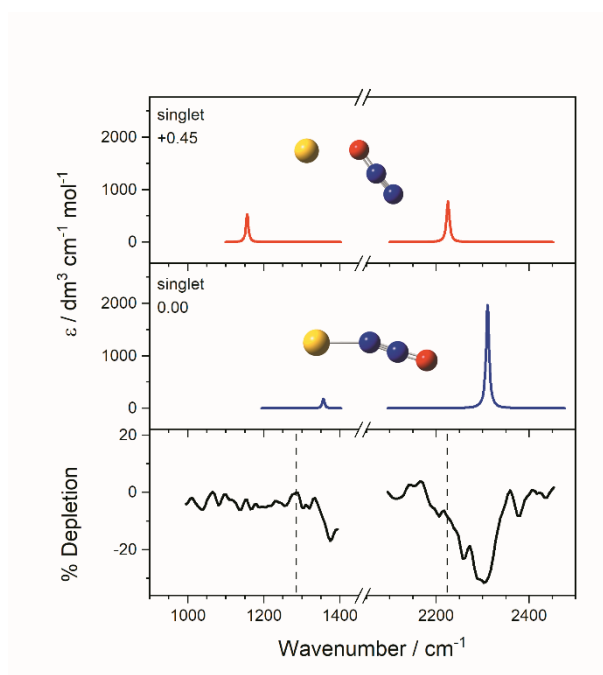
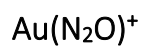


Figure S4. IR-MPD depletion spectrum of $\text{Au}(\text{N}_2\text{O})^+$, along with simulated IR spectra of singlet-state isomers in the region of the N_2O symmetric ($\text{N}=\text{O}$) and asymmetric ($\text{N}=\text{N}$) stretch. Simulated IR bands corresponding to N-bound and O-bound ligands are indicated in blue and red, respectively. The relative energies of different isomers are given in eV. The vertical dashed lines at 1285 and 2224 cm^{-1} indicate the wavenumber of the $\nu_1(\text{N}=\text{O})$ and $\nu_3(\text{N}=\text{N})$ modes in isolated N_2O , respectively.¹

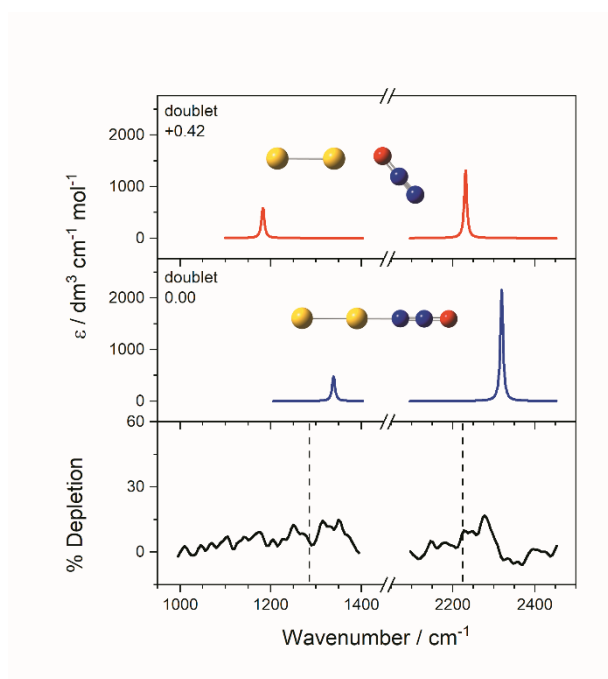
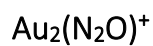


Figure S5. IR-MPD depletion spectrum of $\text{Au}_2(\text{N}_2\text{O})^+$, along with simulated IR spectra of doublet-state isomers in the region of the N_2O symmetric ($\text{N}=\text{O}$) and asymmetric ($\text{N}=\text{N}$) stretch. Simulated IR bands corresponding to N-bound and O-bound ligands are indicated in blue and red, respectively. The relative energies of different isomers are given in eV. The vertical dashed lines at 1285 and 2224 cm^{-1} indicate the wavenumber of the $\nu_1(\text{N}=\text{O})$ and $\nu_3(\text{N}=\text{N})$ modes in isolated N_2O , respectively.¹

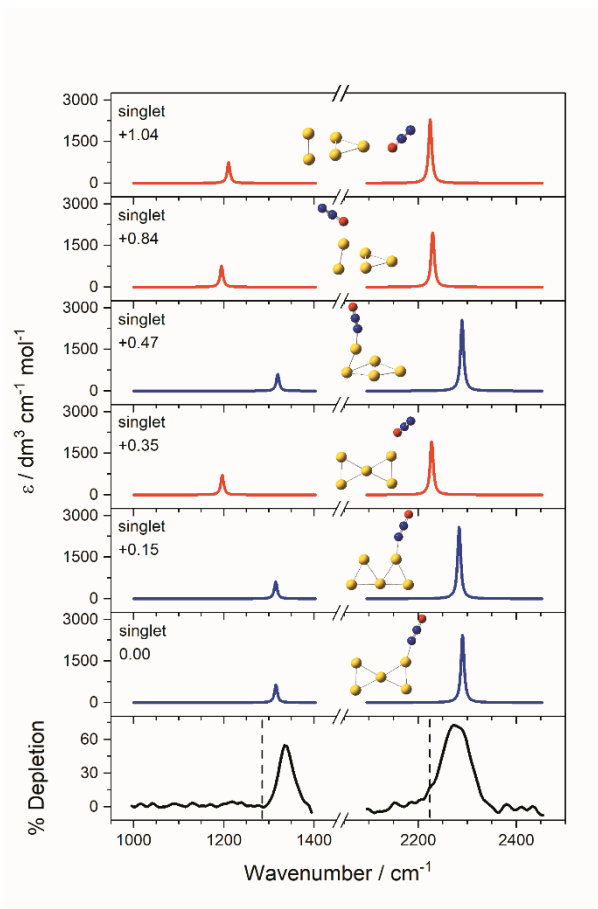
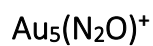


Figure S6. IR-MPD depletion spectrum of $\text{Au}_5(\text{N}_2\text{O})^+$, along with simulated IR spectra of singlet-state isomers in the region of the N_2O symmetric ($\text{N}=\text{O}$) and asymmetric ($\text{N}=\text{N}$) stretch. Simulated IR bands corresponding to N-bound and O-bound ligands are indicated in blue and red, respectively. The relative energies of different isomers are given in eV. The vertical dashed lines at 1285 and 2224 cm^{-1} indicate the wavenumber of the $\nu_1(\text{N}=\text{O})$ and $\nu_3(\text{N}=\text{N})$ modes in isolated N_2O , respectively.¹

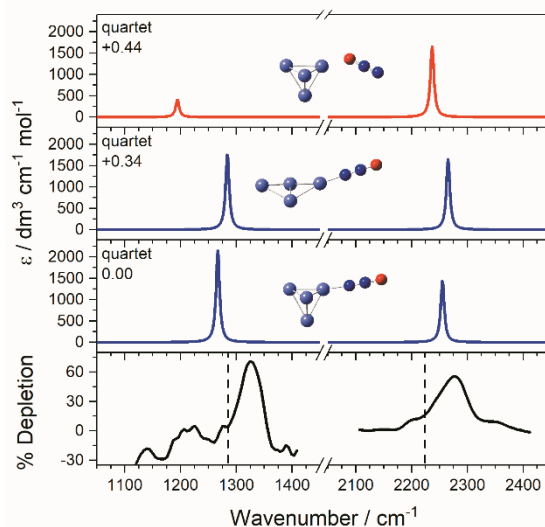
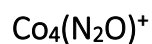


Figure S7. IR-MPD depletion spectrum of $\text{Co}_4(\text{N}_2\text{O})^+$, along with simulated IR spectra of quartet-state isomers in the region of the N_2O symmetric ($\text{N}=\text{O}$) and asymmetric ($\text{N}=\text{N}$) stretch. Simulated IR bands corresponding to N-bound and O-bound ligands are indicated in blue and red, respectively. The relative energies of different isomers are given in eV. The vertical dashed lines at 1285 and 2224 cm^{-1} indicate the wavenumber of the $\nu_1(\text{N}=\text{O})$ and $\nu_3(\text{N}=\text{N})$ modes in isolated N_2O , respectively.¹

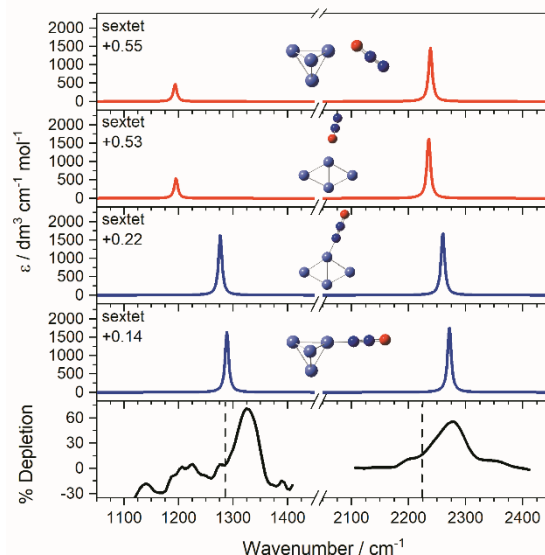


Figure S8. IR-MPD depletion spectrum of $\text{Co}_4(\text{N}_2\text{O})^+$, along with simulated IR spectra of sextet-state isomers in the region of the N_2O symmetric ($\text{N}=\text{O}$) and asymmetric ($\text{N}=\text{N}$) stretch. Simulated IR bands corresponding to N-bound and O-bound ligands are indicated in blue and red, respectively. The relative energies of different isomers are given in eV. The vertical dashed lines indicate the wavenumber of the $\nu_1(\text{N}=\text{O})$ and $\nu_3(\text{N}=\text{N})$ modes in isolated N_2O .¹

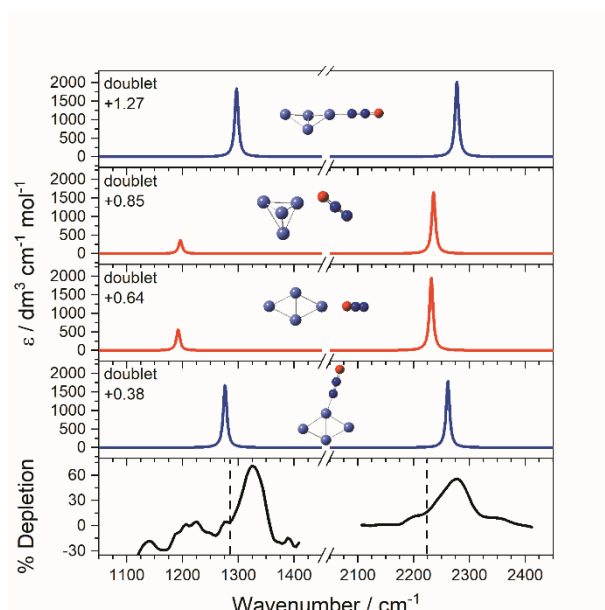


Figure S9. IR-MPD depletion spectrum of $\text{Co}_4(\text{N}_2\text{O})^+$, along with simulated IR spectra of doublet-state isomers in the region of the N_2O symmetric ($\text{N}=\text{O}$) and asymmetric ($\text{N}=\text{N}$) stretch. Simulated IR bands corresponding to N-bound and O-bound ligands are indicated in blue and red, respectively. The relative energies of different isomers are given in eV. The vertical dashed lines indicate the wavenumber of the $\nu_1(\text{N}=\text{O})$ and $\nu_3(\text{N}=\text{N})$ modes in isolated N_2O .¹

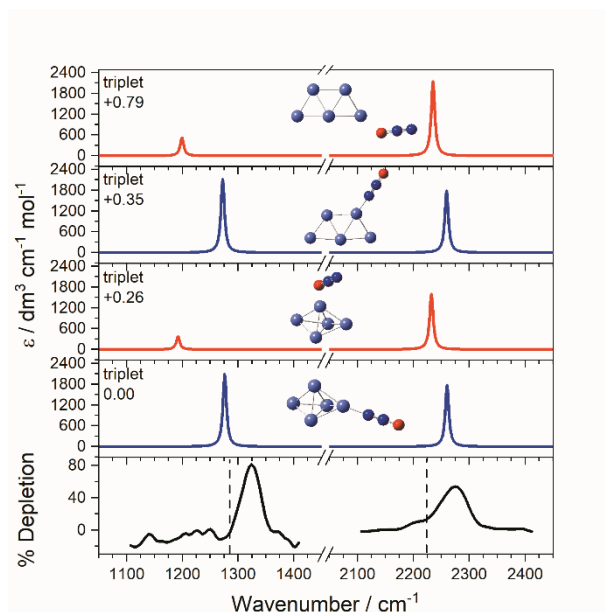
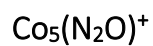


Figure S10. IR-MPD depletion spectrum of $\text{Co}_5(\text{N}_2\text{O})^+$, along with simulated IR spectra of triplet-state isomers in the region of the N_2O symmetric ($\text{N}=\text{O}$) and asymmetric ($\text{N}=\text{N}$) stretch. Simulated IR bands corresponding to N-bound and O-bound ligands are indicated in blue and red, respectively. The relative energies of different isomers are given in eV. The vertical dashed lines at 1285 and 2224 cm^{-1} indicate the wavenumber of the $\nu_1(\text{N}=\text{O})$ and $\nu_3(\text{N}=\text{N})$ modes in isolated N_2O , respectively.¹

Calculated Structures

Density functional theory calculations were performed employing the TPSSh functional and Def2TZVP basis set using the Gaussian09 package.² The quadratically convergent SCF procedure was used along with 1.00D-06 hartree convergence criterion along with the Gaussian 09 “Very tight” geometry optimisation convergence. For each cluster, starting structures were generated from existing calculations of cationic gold³ and cobalt clusters.⁴ To accurately determine the multiplicity of each cluster structure, together with the relative energy, for each calculated structure the DFT wavefunction was stabilised and tested. For each structure, cartesian coordinates (Å) along with relative energies (eV) are given.

The adsorption of N₂O has minimal effect on the relative ordering of different isomers and/or spin states of Au_n⁺ and Co_n⁺ clusters. Likewise, the geometrical structure of the metal cluster substrate does not change significantly upon N₂O binding.

Au_n(N₂O)⁺

Au₂(N₂O)⁺

2S+1 = 2;

Lowest energy structure: N-bound

Au 0.874428 1.676623 -0.062429
Au 0.254200 -0.844890 0.030750
N -0.506522 -3.932270 0.144275
N -0.237823 -2.838562 0.105644
O -0.784222 -5.060540 0.184882

O-bound, E_{rel} = 0.42 eV

Au 2.114280 0.064210 0.053901
Au -0.481459 -0.038961 0.193372
N 5.139367 0.017670 0.694152
N 5.931002 -0.115804 1.470788
O 4.324730 0.171398 -0.187455

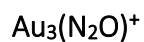
2S+1 = 4;

N-bound, E_{rel} = 3.07 eV

Au 1.523270 -0.326430 0.000000
Au -1.138327 0.024615 0.000000
N 1.817842 -3.471001 0.000000
N 1.127845 -2.564748 0.000000
O 2.498833 -4.412690 0.000000

O-bound, E_{rel} = 3.19 eV

Au 1.695813 0.013021 -0.852664
Au -0.489515 0.181837 0.701870
N 3.715904 2.285711 0.232003
N 4.712455 2.740247 0.004289
O 2.637685 1.807120 0.491356



2S+1 = 1;

Lowest energy structure: N-bound

Au 0.978731 0.054944 0.142263
 Au -1.655903 -0.127305 -0.094605
 Au -0.235497 -2.288859 -0.107521
 N 3.650581 1.804344 0.486500
 N 2.711437 1.192416 0.361983
 O 4.619853 2.436322 0.614426

O-bound, E_{rel} = 0.38 eV

Au 1.893078 0.607970 0.550879
 Au -0.724286 0.537189 0.215993
 Au 0.721316 -1.496076 -0.530981
 N 4.456670 2.373236 0.721902
 N 5.147030 3.072596 0.189650
 O 3.738466 1.621754 1.337590

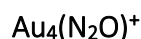
2S+1 = 3;

N-bound, E_{rel} = 2.16 eV

Au 1.311711 -0.510826 0.151055
 Au -1.191494 0.363475 -0.038705
 Au -0.504386 -2.224837 -0.133089
 N 3.469053 1.812347 0.473159
 N 2.836602 0.883765 0.367010
 O 4.147715 2.747937 0.583616

O-bound, E_{rel} = 2.53 eV

Au 1.373311 -0.508117 0.216635
 Au -1.091723 0.439026 0.265988
 Au -0.461690 -2.042506 -0.549300
 N 3.428216 1.765406 0.467945
 N 3.804084 2.736610 0.065771
 O 3.063006 0.713409 0.946067



$2S+1 = 2;$

Lowest energy structure: N-bound

Au 1.160947 -0.935873 1.896374
 Au -0.261433 0.717857 0.263284
 Au 0.800216 -1.558901 -0.642098
 Au -0.551801 -0.052241 -2.333246
 N -1.296651 3.579156 1.338104
 N -1.071355 2.530186 0.987736
 O -1.546279 4.657134 1.703273

N-bound, $E_{\text{rel}} = 0.11 \text{ eV}$

Au 1.227001 -0.002017 0.001885
 Au -1.429466 -0.055851 0.000220
 Au -0.001582 -2.361277 -0.012172
 Au -0.217327 2.287859 0.014589
 N -0.187998 5.506802 0.039503
 N 0.054920 4.403562 0.027996
 O -0.415995 6.649200 0.051118

N-bound, $E_{\text{rel}} = 0.14 \text{ eV}$

Au 0.768360 0.009021 2.733285
 Au -0.317841 -0.005789 0.348866
 Au 1.133122 0.011860 -1.888760
 Au -1.489556 -0.019491 -1.992387
 N 3.947385 0.027081 -3.431635
 N 3.019700 0.032216 -2.789661
 O 4.914225 0.023231 -4.082886

N-bound, $E_{\text{rel}} = 0.15 \text{ eV}$

Au 0.869300 -0.920374 3.332136
 Au 0.250161 -0.171749 0.903263
 Au 1.088323 -0.790473 -1.487806
 Au -0.803108 0.977435 -1.330567
 N -3.104574 3.135832 -1.952502
 N -2.282368 2.391944 -1.747881
 O -3.952533 3.906767 -2.166458

N-bound, $E_{\text{rel}} = 0.34 \text{ eV}$

Au 0.040943 -0.092977 3.041909
 Au -0.627831 -0.168547 0.549350
 Au 1.290214 0.350431 -1.183129
 Au -1.062661 -0.149165 -2.149076
 N 0.239831 -0.230453 6.227411
 N 0.374086 -0.102852 5.114173
 O 0.124024 -0.354859 7.381654

O-bound, $E_{\text{rel}} = 0.34 \text{ eV}$

Au -0.069191 -0.007568 0.444222
 Au -0.734784 0.284083 -2.135662
 Au -0.970581 -2.098570 -1.003225
 Au 0.181854 2.376419 -0.795111
 N -0.099595 -0.148954 3.620143
 N -0.712612 -0.041700 4.549580
 O 0.590296 -0.272742 2.639349

O-bound, $E_{\text{rel}} = 0.39 \text{ eV}$

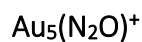
Au 1.238642 -0.153588 0.301172
 Au -1.363303 -0.007318 -0.290254
 Au -0.178301 -2.397293 -0.064948
 Au 0.046621 2.217734 0.103489
 N 0.343891 5.319027 -0.579053
 N 0.562626 6.071082 -1.377948
 O 0.104649 4.531879 0.301553

O-bound, $E_{\text{rel}} = 0.52 \text{ eV}$

Au -1.088406 0.227356 3.230095
 Au -0.056739 0.076611 0.831774
 Au 1.377898 0.041338 -1.453942
 Au -1.194307 -0.279630 -1.505711
 N 4.357075 -0.529086 -2.222568
 N 5.128442 -1.314205 -2.420169
 O 3.555193 0.348349 -2.017505

O-bound, $E_{\text{rel}} = 0.66 \text{ eV}$

Au -0.077982 0.237899 2.833624
 Au -0.536120 0.079542 0.287347
 Au 1.369038 -0.324689 -1.498333
 Au -1.071948 -0.062781 -2.353787
 N -0.553034 0.602491 5.979132
 N -1.307392 0.806348 6.780331
 O 0.281643 0.381244 5.141229



$2S+1 = 1;$

Lowest energy structure: N-bound

Au 0.452100 -1.896035 -0.187487
 Au -1.765437 -0.316820 -0.043206
 Au -1.903526 -2.919289 -0.366365
 Au -1.425072 2.314007 0.279075
 Au -3.831830 1.386486 0.131834
 N 3.654180 -1.690310 -0.090950
 N 2.527655 -1.636347 -0.107922
 O 4.820345 -1.731443 -0.071347

N-bound, $E_{\text{rel}} = 0.15$ eV

Au -0.556657 -2.156457 -0.250405
 Au -2.965701 -0.922389 -0.258584
 Au -2.722507 -3.546098 -0.648802
 Au -0.883051 0.774738 0.178535
 Au -3.364731 1.623065 0.106026
 N 2.099235 1.798290 0.583818
 N 1.143443 1.220541 0.416471
 O 3.099694 2.372655 0.754304

O-bound, $E_{\text{rel}} = 0.35$ eV

Au 0.172853 -2.153535 -0.215258
 Au -1.831813 -0.352375 -0.067300
 Au -2.262769 -2.919103 -0.540184
 Au -1.287384 2.230181 0.354000
 Au -3.755791 1.502289 0.119645
 N 3.124329 -2.623075 0.744948
 N 3.775406 -3.125024 1.503636
 O 2.455495 -2.068736 -0.090191

N-bound $E_{\text{rel}} = 0.47$ eV

Au -0.280043 0.029119 -2.817395
 Au -0.313926 1.313937 -0.480129
 Au -0.318968 -1.305447 -0.508221
 Au -1.105182 -0.020022 1.888657
 Au 1.428726 -0.020416 1.422691
 N 4.582746 -0.044714 1.925480
 N 3.514967 -0.027777 1.560685
 O 5.692712 -0.061151 2.281457

O-bound, $E_{\text{rel}} = 0.83$ eV

Au -0.438671 0.352680 -2.845909
 Au -0.121622 1.385771 -0.408808
 Au -0.511408 -1.193096 -0.675314
 Au -1.114137 -0.034452 1.855197
 Au 1.386654 -0.354948 1.338618
 N 4.332166 -0.883056 2.240001
 N 5.006054 -1.070068 3.112549
 O 3.639011 -0.683828 1.273395

O-bound, $E_{\text{rel}} = 1.04$ eV

Au -0.078986 0.035986 -2.687095
 Au -0.055243 1.301394 -0.337580
 Au 0.058431 -1.296484 -0.378782
 Au -1.235845 -0.088089 1.924418
 Au 1.332198 0.024655 1.874744
 N 0.620586 0.122325 -5.897559
 N 1.438944 0.174631 -6.660746
 O -0.269135 0.065908 -5.093617

$\text{Co}_n(\text{N}_2\text{O})^+$

$\text{Co}_2(\text{N}_2\text{O})^+$

$2S+1 = 6;$

Lowest energy structure: N-bound

Co -2.373164 0.046364 0.044090
Co -0.119900 0.002296 0.002276
N 2.997270 -0.058498 -0.055739
N 1.867351 -0.036505 -0.034668
O 4.157547 -0.081099 -0.077377

O-bound, $E_{\text{rel}} = 0.24$ eV

Co 2.244857 0.271635 0.000044
Co 0.090882 -0.346913 -0.000098
N -2.925322 0.154474 0.000050
N -3.821670 0.819435 -0.000063
O -1.979498 -0.598107 0.000195

$2S+1 = 4;$

N-bound, $E_{\text{rel}} = 0.70$ eV

Co -0.060379 -0.099999 0.564067
Co 0.379553 1.222030 -1.394993
N -1.002824 -2.946469 0.312544
N -0.648386 -1.876661 0.415363
O -1.368221 -4.049643 0.203203

O-bound, $E_{\text{rel}} = 1.11$ eV

Co 0.102087 -1.631681 0.698892
Co -0.042557 0.673725 0.322116
N -0.197784 3.434783 -0.889853
N -0.226035 4.150371 -1.747209
O -0.170665 2.702171 0.070055

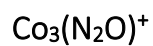
$2S+1 = 2;$

N-bound, $E_{\text{rel}} = 0.05$ eV

Co 0.099783 0.100210 -0.000065
Co 2.392819 -0.064494 0.000002
N -2.996311 -0.040372 0.000376
N -1.866900 0.013459 0.000256
O -4.157223 -0.096995 -0.000339

O-bound, $E_{\text{rel}} = 0.24$ eV

Co -0.067501 0.254974 1.102051
Co 0.190821 -0.423694 -1.103573
N 0.204537 1.018960 -3.827746
N 0.538341 1.838644 -4.507653
O -0.178455 0.117904 -3.117447



2S+1 = 3;

Lowest energy structure, N-bound

Co 1.575679 0.069304 0.049642
 Co -0.504369 1.371541 0.055138
 Co -0.533627 -1.020656 -0.064426
 N 4.440020 -0.936850 0.082329
 N 3.366950 -0.575866 0.072843
 O 5.546951 -1.314326 0.088899

O-bound, $E_{\text{rel}} = 0.44$ eV

Co 1.395776 0.232667 -0.264279
 Co -0.716613 1.216524 0.429564
 Co -0.468535 -1.140799 0.073444
 N 4.239433 -0.693564 -0.666564
 N 5.067611 -1.429481 -0.517134
 O 3.371411 0.122174 -0.852217

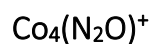
2S+1 = 5;

N-bound, $E_{\text{rel}} = 0.68$ eV

Co 0.491853 -1.583491 0.123532
 Co 0.587800 0.704444 -0.114093
 Co -1.529211 -0.404188 0.059973
 N 3.220528 2.143493 -0.320428
 N 2.228856 1.601445 -0.242708
 O 4.246604 2.701496 -0.398550

O-bound, $E_{\text{rel}} = 1.02$ eV

Co 1.207019 -0.719418 -0.341658
 Co 0.253780 1.347207 -0.055626
 Co -1.024546 -0.546351 0.380388
 N 4.214543 -0.821420 0.105887
 N 5.165874 -0.373105 0.482897
 O 3.204319 -1.334368 -0.308797



2S+1 = 4;

Lowest energy structure: N-bound

Co 0.659469 -0.711715 -0.092536
 Co 0.041795 1.449723 -0.790058
 Co -0.657733 0.661856 1.310686
 Co -1.726272 -0.347852 -0.637039
 N 1.772315 -3.142761 1.327923
 N 1.313635 -2.232299 0.833155
 O 2.237782 -4.083601 1.850117

N-bound, $E_{\text{rel}} = 0.34$ eV

Co -0.138825 1.010750 1.242706
 Co -2.190656 -0.168503 1.346392
 Co 1.375502 0.189512 -0.541535
 Co -0.200003 -1.259612 0.725401
 N 3.456071 0.620564 -2.722104
 N 2.672721 0.468830 -1.918638
 O 4.265596 0.779379 -3.553225

O-bound, $E_{\text{rel}} = 0.44$ eV

Co 1.713639 -0.048260 0.077123
 Co -0.097484 0.753393 -1.183208
 Co -0.390153 0.548777 1.250411
 Co -0.179406 -1.387500 -0.261015
 N 4.252188 -0.755491 -1.260397
 N 4.787273 -1.194294 -2.138333
 O 3.711737 -0.273060 -0.296470

2S+1 = 6;

N-bound, $E_{\text{rel}} = 0.14$ eV

Co 0.886392 0.315886 -0.235432
 Co -0.954737 0.335488 1.202932
 Co -1.392732 0.244693 -1.162406
 Co -0.346472 -1.665675 -0.054997
 N 3.872362 0.352021 0.334781
 N 2.758347 0.326416 0.137781
 O 5.023023 0.374209 0.541324

N-bound, $E_{\text{rel}} = 0.22$ eV

Co -0.286694 1.057427 -0.096919
 Co 0.145856 0.428220 2.105015
 Co 0.179082 -0.374338 -1.922370
 Co 0.043686 -1.346945 0.373700
 N 0.098040 -4.320932 -0.221808
 N 0.077565 -3.198739 -0.068205
 O 0.119520 -5.480248 -0.391073

O-bound, $E_{\text{rel}} = 0.53$ eV

Co -0.061210 1.120300 0.003539
 Co 0.162894 0.003070 2.164542
 Co -0.032974 0.052655 -2.106057
 Co 0.011221 -1.184815 -0.012966
 N 0.885336 -4.032645 -0.675545
 N 1.672955 -4.774688 -0.956256
 O 0.010889 -3.259330 -0.373690

O-bound, $E_{\text{rel}} = 0.55$ eV

Co 0.745241 -0.726895 -1.400429
 Co 0.141400 1.389147 -0.346635
 Co 0.684361 -0.496863 0.908671
 Co -1.416698 -0.495586 -0.357560
 N 3.050994 0.040844 2.630509
 N 3.956513 0.651137 2.867104
 O 2.082032 -0.643146 2.409343

2S+1 = 2;

N-bound, $E_{\text{rel}} = 0.38\text{eV}$

Co -0.769319 1.013692 0.121068
Co -1.377360 -0.150355 2.118710
Co 1.343416 0.262341 -0.471845
Co -0.245693 -1.233546 0.313041
N 3.613726 0.617095 -2.470971
N 2.779456 0.489191 -1.718230
O 4.473756 0.748992 -3.249518

O-bound, $E_{\text{rel}} = 0.64\text{ eV}$

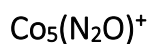
Co 1.241366 -0.413188 -0.912526
Co -0.285204 1.352501 -0.254034
Co 0.583083 -0.221854 1.401669
Co -1.111305 -0.890074 -0.557760
N 4.198365 -0.723217 -1.022689
N 5.192015 -0.764522 -0.511458
O 3.147625 -0.679815 -1.611920

O-bound, $E_{\text{rel}} = 0.85\text{ eV}$

Co -0.357347 1.089751 0.041376
Co 0.378549 -0.001022 2.136201
Co -0.126183 0.051004 -2.189016
Co 0.007817 -1.142557 -0.022312
N 0.662213 0.297132 -5.125101
N 1.424524 0.486428 -5.920970
O -0.183640 0.088297 -4.291891

N-bound, $E_{\text{rel}} = 1.27\text{ eV}$

Co -1.456703 0.546271 0.127336
Co 0.167337 0.219229 1.888429
Co -0.746945 0.679769 -2.111731
Co 0.806484 -0.260490 -0.388452
N 3.536198 -1.547799 -0.095576
N 2.514205 -1.062194 -0.145533
O 4.593215 -2.049193 -0.032401



2S+1 = 3;

Lowest energy structure: N-bound

Co -0.058773 -0.078146 1.313855
 Co -2.042833 0.196078 -0.087908
 Co -0.065504 -1.104534 -0.870827
 Co 2.005239 -0.221671 0.115387
 Co 0.130993 1.319055 -0.633960
 N -4.944333 -0.362595 0.677220
 N -3.862510 -0.171386 0.404071
 O -6.062176 -0.563838 0.965021

O-bound, $E_{\text{rel}} = 0.26$ eV

Co -0.297084 -0.536656 1.229458
 Co -1.810636 -0.138113 -0.711750
 Co 0.460908 -0.829759 -0.997394
 Co 1.971585 0.210980 0.616850
 Co 0.014299 1.360329 -0.249591
 N 0.004797 -3.113387 -2.807190
 N -0.691366 -3.832576 -3.306090
 O 0.789614 -2.359785 -2.288853

N-bound, $E_{\text{rel}} = 0.35$ eV

Co -3.180375 1.540343 -0.638097
 Co -4.701338 0.129470 0.468335
 Co -2.334262 -0.407642 0.230471
 Co -0.754163 1.525739 0.113141
 Co 0.046488 -0.683045 -0.280133
 N 1.226366 3.783749 0.554686
 N 0.506571 2.925490 0.388344
 O 1.976204 4.668659 0.726329

O-bound, $E_{\text{rel}} = 0.79$ eV

Co -3.314043 1.698354 -0.298918
 Co -4.603816 -0.214716 0.400611
 Co -2.175230 -0.393674 -0.188810
 Co -0.887674 1.574211 0.298871
 Co 0.210384 -0.528306 -0.268406
 N -7.433291 -1.193805 1.077186
 N -8.531145 -1.011017 1.188808
 O -6.255445 -1.418035 0.962673

2S+1 = 5;

N-bound, $E_{\text{rel}} = 0.48$ eV

Co 0.098564 -0.135294 1.333523
 Co -2.024912 0.401497 0.326531
 Co -0.404217 -1.110035 -0.803032
 Co 1.819556 -0.470314 -0.256301
 Co 0.076194 1.319703 -0.598533
 N -0.121118 -3.654708 -2.350952
 N -0.187639 -2.686192 -1.766298
 O -0.043110 -4.657097 -2.958552

O-bound, $E_{\text{rel}} = 0.72$ eV

Co -0.493648 0.353257 1.182289
 Co -1.981608 -0.540909 -0.435112
 Co 0.269846 -1.479111 -0.368230
 Co 1.723183 0.444323 0.285079
 Co -0.200318 0.893256 -1.066929
 N -4.670614 0.672016 -0.478346
 N -5.311751 1.576355 -0.331092
 O -4.009980 -0.321603 -0.645936

N-bound, $E_{\text{rel}} = 0.93$ eV

Co -3.835393 1.476621 -0.180192
 Co -4.657221 -0.805467 0.223744
 Co -2.380363 -0.409189 0.024968
 Co -1.432505 1.801042 0.218938
 Co -0.001582 0.004521 -0.183319
 N -4.458703 4.368424 -0.788760
 N -4.144794 3.305325 -0.550887
 O -4.771437 5.471822 -1.033861

O-bound, $E_{\text{rel}} = 1.31$ eV

Co -3.248768 1.642834 -0.625844
 Co -4.762602 -0.156876 -0.366009
 Co -2.360929 -0.390553 -0.034243
 Co -1.039273 1.467393 0.588442
 Co 0.080962 -0.588175 0.229190
 N -7.227377 -1.154942 1.155458
 N -7.774965 -1.297777 2.120074
 O -6.657307 -1.008893 0.104947

Bond Lengths

(N₂O)

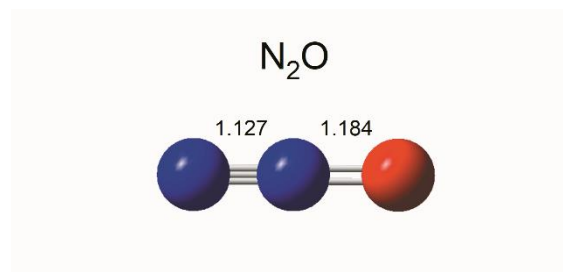


Figure S11. Bond lengths (Å) of N₂O calculated at the TPSSh/Def2TZVP level of theory.

The experimental bond lengths¹ of nitrous oxide are presented also for comparison:

$$r(\text{N}=\text{N}): 1.128 \text{ Å}$$

$$r(\text{N}=\text{O}): 1.184 \text{ Å}$$

Au_n(N₂O)⁺

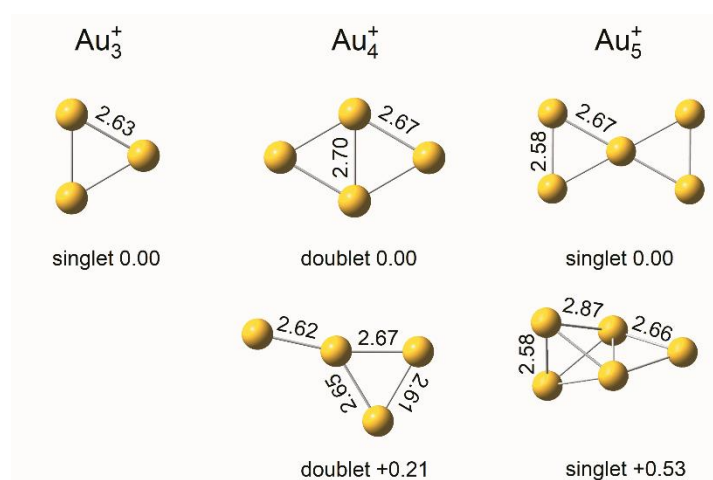


Figure S12. Low-lying isomers of Au_n⁺ (*n* = 3-5) clusters calculated at the TPSSh/Def2TZVP level of theory. Energies are given in eV and distances in angstroms.

Table S1. Bond lengths (Å) of the calculated $\text{Au}_n(\text{N}_2\text{O})^+$ structures, employing TPSSh functional and Def2TZVP basis set. In this case, N1 represents the terminal N atom and Au represents the gold atom bound to the N_2O molecule (either N- or O-bound).

Isomer	Au-N1	Au-O	N=N	N=O
$^1\text{AuNNO}^+$	2.034	---	1.130	1.157
$^1\text{AuONN}^+$	---	2.187	1.115	1.218
$^2\text{Au}_2\text{NNO}^+$	2.055	---	1.127	1.163
$^2\text{Au}_2\text{ONN}^+$	---	2.226	1.117	1.210
$^1\text{Au}_3\text{NNO}^+$	2.084	---	1.128	1.164
$^1\text{Au}_3\text{ONN}^+$	---	2.248	1.118	1.208
$^2\text{Au}_4\text{NNO}^+$	2.113	---	1.129	1.165
$^2\text{Au}_4\text{ONN}^+$	---	2.307	1.119	1.206
$^1\text{Au}_5\text{NNO}^+$	2.093	---	1.128	1.167
$^1\text{Au}_5\text{ONN}^+$	---	2.287	1.119	1.205

Co_n(N₂O)⁺

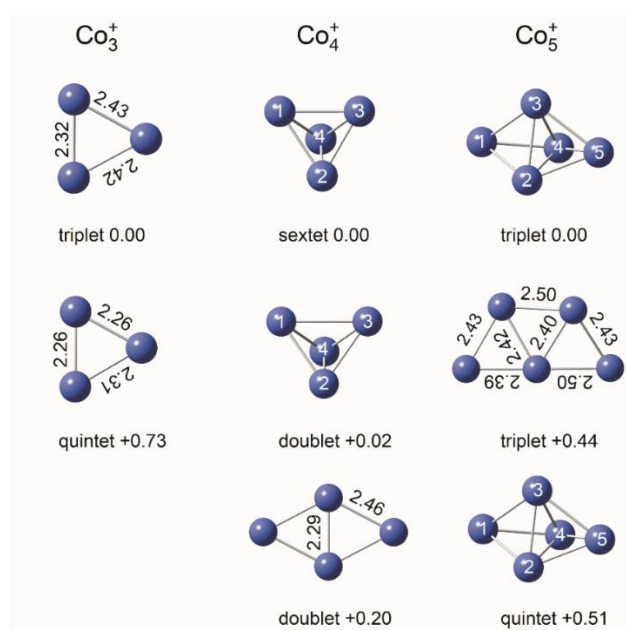


Figure S13. Low-lying isomers of Co_n⁺ (*n* = 3-5) clusters calculated at the TPSSh/Def2TZVP level of theory. Energies are given in eV and distances in angstroms.

Table S2. Bond lengths (Å) of calculated non-planar ^{6/2}Co₄⁺ clusters, whereby title integers represent atom labels presented in Figure S13.

Cobalt Cluster	1-2	1-3	1-4	2-3	2-4	3-4
⁶ Co ₄ ⁺	2.41	2.45	2.45	2.45	2.38	2.29
² Co ₄ ⁺	2.43	2.73	2.41	2.45	2.41	2.41

Table S3. Bond lengths (Å) of calculated non-planar ^{3/5}Co₅⁺ clusters, whereby title integers represent atom labels presented in Figure S13.

Cobalt Cluster	1-2	1-3	1-4	2-3	2-4	3-4	2-5	3-5	4-5
³ Co ₅ ⁺	2.40	2.48	2.49	2.41	2.40	2.50	2.39	2.46	2.56
⁵ Co ₅ ⁺	2.40	2.53	2.38	2.43	2.43	2.56	2.40	2.53	2.38

Table S4. Bond lengths (Å) of the calculated $\text{Co}_n(\text{N}_2\text{O})^+$ structures, employing TPSSh functional and Def2TZVP basis set. In this case, N1 represents the terminal N atom and Co represents the cobalt atom bound to the N_2O molecule (either N- or O-bound).

Isomer	Co-N1	Co-O	N=N	N=O
$^3\text{CoNNO}^+$	1.879	---	1.131	1.162
$^3\text{CoONN}^+$	---	1.993	1.116	1.212
$^6\text{Co}_2\text{NNO}^+$	1.988	---	1.130	1.161
$^6\text{Co}_2\text{ONN}^+$	---	2.086	1.116	1.209
$^3\text{Co}_3\text{NNO}^+$	1.904	---	1.132	1.170
$^3\text{Co}_3\text{ONN}^+$	---	2.068	1.117	1.207
$^4\text{Co}_4\text{NNO}^+$	1.914	---	1.132	1.171
$^4\text{Co}_4\text{ONN}^+$	---	2.045	1.118	1.206
$^3\text{Co}_5\text{NNO}^+$	1.941	---	1.131	1.171
$^3\text{Co}_5\text{ONN}^+$	---	2.082	1.118	1.204

References

- (1) Herzberg, G. *Molecular Spectra and Molecular Structure: II Infrared and Raman Spectra of Polyatomic Molecules*; Krieger: Malabar, Florida, 1991; Vol. 2.
- (2) Frisch, M. J.; Trucks, G. W.; Schlegel, H. B.; Scuseria, G. E.; Robb, M. A.; Cheeseman, J. R.; Scalmani, G.; Barone, V.; Mennucci, B.; Petersson, G. A.; Nakatsuji, H.; Caricato, M.; Li, X.; Hratchian, H. P.; Izmaylov, A. F.; Bloino, J.; Zheng, G.; Sonnenberg, J. L.; Hada, M.; Ehara, M.; Toyota, K.; Fukuda, R.; Hasegawa, J.; Ishida, M.; Nakajima, T.; Honda, Y.; Kitao, O.; Nakai, H.; Vreven, T.; Montgomery, J. A.; Peralta, J. E.; Ogliaro, F.; Bearpark, M.; Heyd, J. J.; Brothers, E.; Kudin, K. N.; Staroverov, V. N.; Kobayashi, R.; Normand, J.; Raghavachari, K.; Rendell, A.; Burant, J. C.; Iyengar, S. S.; Tomasi, J.; Cossi, M.; Rega, N.; Millam, J. M.; Klene, M.; Knox, J. E.; Cross, J. B.; Bakken, V.; Adamo, C.; Jaramillo, J.; Gomperts, R.; Stratmann, R. E.; Yazyev, O.; Austin, A. J.; Cammi, R.; Pomelli, C.; Ochterski, J. W.; Martin, R. L.; Morokuma, K.; Zakrzewski, G.; Voth, G. A.; Salvador, P.; Dannenberg, J. J.; Dapprich, S.; Daniels, A. D.; Farkas, O.; Foresman, J. B.; Ortiz, J. V.; Cioslowski, J.; Fox, D. J. *Gaussian 09, Revision D.01*; Gaussian, Inc.: Wallingford CT, 2009.
- (3) Gilb, S.; Weis, P.; Furche, F.; Ahlrichs, R.; Kappes, M. M. Structures of Small Gold Cluster Cations (Au_n^+ , $N < 14$): Ion Mobility Measurements versus Density Functional Calculations. *J. Chem. Phys.* **2002**, *116* (10), 4094–4101.
- (4) Gehrke, R.; Gruene, P.; Fielicke, A.; Meijer, G.; Reuter, K. Nature of Ar Bonding to Small Co_n^+ Clusters and Its Effect on the Structure Determination by Far-Infrared Absorption Spectroscopy. *J. Chem. Phys.* **2009**, *130* (3), 034306.